The existence of strange nonchaotic attractors in the quasiperiodically forced Ricker family

Gaolei Li[a,b] **Yuan Yue**[a,b] [1] **Denghui Li**[c] **Jianhua Xie**[a] **Celso Grebogi**[d]

[a]*School of Mechanics and Engineering, Southwest Jiaotong University, Chengdu 610031, PR China*

[b]*Applied Mechanics and Structure Safety Key Laboratory of Sichuan Province, Southwest Jiaotong University, Chengdu, Sichuan 610031, PR China*

[c]*School of Mathematics and Statistics, Hexi University, Zhangye 734000, China*

[d]*Institute for Complex Systems and Mathematical Biology King's College, University of Aberdeen, Aberdeen AB24 3UE, United Kingdom*

Abstract

In this paper, the Ricker family (a population model) with quasiperiodic excitation is considered. The existence of strange nonchaotic attractors (SNAs) is analyzed in a co-dimension-2 parameter space by both theory and numerical methods. We prove that SNAs exist in a positive measure parameter set. The SNAs are nowhere differentiable (i.e. strange). We use numerical methods to identify the existence of SNAs in a larger parameter set. The nonchaotic property of SNAs is verified by evaluating the Lyapunov exponents, while the strange property is characterized by phase sensitivity and rational approximations. We also find that there is a transition region in parameter plane in which SNAs alternate with chaotic attractors.

Keywords: Strange nonchaotic attractors; Lyapunov exponent; Phase sensitivity; Rational approximations

1. Introduction

In dynamical systems, the types of attractors include periodic attractors, quasiperiodic attractors and chaotic attractors. Strange nonchaotic attractor is considered as the fourth type of attractor. It has been uncovered by Grebogi et al. [1] in 1984. An SNA has fractal structure, but is nonchaotic in the dynamical sense. Pikovsky and Feudel [2] introduced the methods of phase sensitivity, phase sensitivity exponent and rational approximations to characterize the strange property of SNAs. In recent years there has been increasing interest in studying SNAs for different classes of dynamical systems.

Numerical simulations have usually been the methods to characterize SNAs in dynamical systems. In that regard, Jalnine et al. [3] verified the existence of SNAs in an autonomous systems by numerical methods, and found that SNAs have singular continuous power spectrum and fractal dimension. Zhang [4] verified the existence of Wada basins of SNAs in Duffing oscillator with quasiperiodic excitation and showed that the domain of SNAs is a complete Wada basin in a parameter set of positive measure. Jorba et al. [5] found that SNAs appear during a pitchfork bifurcation of invariant curves in a

[1]Correspomding author. *E-mail addresses*: leyuan2003@sina.com(Yuan Yue)

one-dimensional map with quasiperiodic excitation. Zhou et al. [6] studied a nonlinear oscillator with a multistable potential by numerical method and simulator. The Lyapunov exponents are studied by precise numerical methods, and the phenomena of chaotic attractors transforming into SNAs are analyzed. Sivaganesh et al. [7] presented a numerical investigation on the robust synchronization phenomenon, observed in a unidirectionally-coupled quasiperiodically-forced simple nonlinear electronic circuit system, exhibiting SNAs in its dynamics. SNAs in two-dimensional maps have zero Lyapunov exponent in one direction and negative Lyapunov exponent in the other direction [1, 8]. Ding et al [9] also studied quasiperiodically forced systems, showing that the set in parameter space for which the system exhibits SNAs has Cantor-like structure and is enclosed by two critical curves. One of those curves marks the transition from three-frequency quasiperiodic attractors to SNAs; the other marks the transition from SNAs to chaotic attractors.

Many researchers have designed experiments to investigate the occurrence of SNAs in real systems. Ditto et al. [10] carried out the first ever experiment to validate the presence of SNAs in a man-made system. They found SNAs dynamics in the magnetic elastic band bending experiment with two-frequency quasiperiodic excitation, and the scaling behavior of Fourier amplitude spectrum is consistent with the predicted scaling behavior of SNAs. Sathish et al. [11] found that if one uses two square waves in an aperiodic manner as input signal to an oscillator system, the response of the oscillator can produce logical SNAs output controlled by the quasiperiodic forcing.

The theoretical studies of SNAs mainly focused on skew product maps. Keller [12] studied a class of monotone incremental quasiperiodically forced map, and proved the existence of SNAs. Alsedà et al. [13] generalized the results of [12] to unimodal quasiperiodically forced maps; the strictly concave function is very important in the proof. Glendinning et al. [14] studied quasiperiodically forced maps, proved that those systems are sensitive to the initial phase, both on the whole phase space and restricted to the attractor. Jäeger [15] proved the existence of non-continuous invariant graphs (SNAs) in quasiperiodically forced systems, and the topological closure of such graphs is typically a filled-in set, i.e., it consists of a single interval on every fibre.

It has been meaningful to study the mechanism of SNAs generation [16]. Thamilmaran et al. [17] argued that three paths can lead to SNAs, namely Heagy-Hammel path, fractal path and intermittent path, and observed the phenomenon of SNAs in a diode both numerically and experimentally. Heagy et al. [18] studied the Duffing system with two-frequency excitation. They found that a quasiperiodic attractor would wrinkle before it changed to an SNA, which is the conversion to SNAs by the fractal path. Fractal path means that before SNAs are generated, attractors produce a wrinkling shape [19, 20, 21, 22]. Heagy-Hammel paths can generate SNAs by the collision of two stable tori with a unstable torus [23]. Intermittent paths include type-I intermittency and type-III intermittency. Type-I intermittency route is created by the saddle-node bifurcation, and type-III intermittency route is caused by torus-doubling. Before SNAs are generated, there are neither the collision of tori nor wrinkling, though the Lyapunov exponent is less than zero [24, 25, 26]. In addition to these three paths, there is the torus-doubling path [27, 28], bubbling path [29] and merging of bubbles route [30]. In 2015, strange nonchaotic star dynamics has been demonstrated in the RR Lyra Constellation, which further validates the presence of strange nonchaotic phenomena in nature [31]. Zelinka et al. [32] investigated the influence of SNA on the evolutionary synthesis of astroinformatic big data classification. The results show that SNA can provide results qualitatively similar

to classic pseudo-random number generators. Strange nonchaotic dynamical phenomena are also found in periodically forced systems. For example, SNAs are found near the bifurcation points of codimension-2 [33] and codimension-3 [34] in periodically forced vibro-impact systems. Wang et al. [35] studied a random dynamical system with periodic excitation, found that small noise can enhance the robustness of SNAs. SNAs can also be induced by noise in nonquasiperiodic discrete-time maps or in periodically driven flows [36]. Numerical results show that small random noise is incapable of causing characteristic changes in the Lyapunov spectrum, but it can make the attractor geometrically strange by dynamically connecting the original periodic attractor with the chaotic saddle.

In this paper, the Ricker family population model with quasiperiodic excitation is considered. The parameter space, in which SNAs occurs, is obtained by combining theoretical and numerical methods. We prove the existence of SNAs in a positive measure parameter space. Numerically we showed that SNAs exist in a larger parameter region. The chaotic properties of attractors are verified by the evaluation of Lyapunov exponents and power spectra while the strange property of attractors are verified by phase sensitivity and rational approximations. In addition, we show that there exists a transition region in which SNAs alternate with chaotic attractors.

2. The model

We investigate a skew product system $F : \mathbb{S}^1 \times \mathbb{R}^+ \to \mathbb{S}^1 \times \mathbb{R}^+$ defined by

$$(\theta, x) \mapsto (\theta + \omega, f(x)g(\theta)), \tag{1}$$

where ω is a irrational number, $\mathbb{S}^1 = \mathbb{R}/\mathbb{Z}$ denotes the unit circle, and $g(\theta) = \sin(\pi\theta)$. The function

$$f(x) = f_{\alpha,\beta}(x) = \alpha x e^{-\beta x}, \quad \alpha > 1, \beta > 0 \tag{2}$$

is the Ricker family, which is a model in population dynamics.

Let $(x_n, \theta_n) = F^n(x, \theta)$. Because the map (1) is a circle translation in the θ direction, the Lyapunov exponent in the θ direction is always zero. The Lyapunov exponent in the x direction is

$$\lambda_x(x, \theta) = \lim_{n\to\infty} \frac{1}{n} \sum_{i=1}^{n} \log \left| \frac{\partial F(x_i, \theta_i)}{\partial x} \right| \tag{3}$$

if the limit exists. Since the map $\theta \mapsto \theta + \omega$ preserves the Lebesgue measure on $\mathbb{S}^1$ and is ergodic, the Lyapunov exponent λ_x at $(0, \theta)$ is

$$\lambda_x(0, \theta) = \int_{\mathbb{S}^1} \log(Df(x)g(\theta))d\theta = \log \alpha - \log 2 \tag{4}$$

for a.e. $\theta \in \mathbb{S}^1$.

From λ_x we can determine that the attractor is either chaotic ($\lambda_x > 0$) or nonchaotic ($\lambda_x < 0$). The derivatives with respect to the phase are infinite everywhere. This implies that the attractors are nonsmooth [1].

3. Existence of SNAs

In this section we prove the existence of an SNA for the map F for a positive measure parameter set. First, we give some preliminary results. Our main Theorem, to be

enunciated and followed by its proof, is based on the following Lemmas [12, 13].

The critical point of $f = f_{\alpha,\beta}(x)$ is $1/\beta$. Let $I = [0, f(1/\beta)]$. Given points $x, y \in I$ with $x \neq y$ (note that $f(x) \neq f(y)$), set

$$\kappa(x,y) = \frac{|x-y|}{\max\{x,y\}} \tag{5}$$

and

$$\tau(x,y) = \frac{\kappa(f(x),f(y))}{\kappa(x,y)}. \tag{6}$$

Note that $|Df(x)| < \frac{f(x)}{x}$ for $x \in (0, 2/\beta)$. We assume $f(1/\beta) < 2/\beta$, that is $\alpha < 2e$.

Lemma 3.1. *Assume that $\alpha < 2e$. For every $\gamma \in (0, f(1/\beta)]$ there exists a constant $\mu < 1$ such that $\tau(x,y) < \mu$ whenever $x, y \in [\gamma, f(1/\beta)]$ and $x \neq y$. In particular, if $x, y \in (0, f(1/\beta)]$ then $\tau(x,y) < 1$.*

Proof. When $\alpha < 2e$, for $x \in (0, f(1/\beta)]$ we have

$$|Df(x)| < \frac{f(x)}{x}. \tag{7}$$

Assume for definiteness that $\gamma \leq x < y \leq f(1/\beta)$. If $f(x) < f(y)$ then

$$\tau(x,y) = \frac{f(y)-f(x)}{y-x}\frac{y}{f(y)} \leq \frac{f(y)-f(\gamma)}{y-\gamma}\frac{y}{f(y)}. \tag{8}$$

By the strict concavity of $f : I \to I$ and $f(0) = 0$, the last expression is smaller than 1. Thus, there exists a constant $\mu_1 < 1$ such that $\tau(x,y) < \mu_1$.

If $f(x) > f(y)$ then $1/\beta < y < f(1/\beta)$ and

$$\tau(x,y) = \frac{f(x)-f(y)}{y-x}\frac{y}{f(x)} < \frac{f(x)-f(y)}{y-x}\frac{y}{f(y)}, \tag{9}$$

which is an increasing function of x by the concavity of f. Thus,

$$\frac{f(x)-f(y)}{y-x}\frac{y}{f(y)} \leq \lim_{x \nearrow y} \frac{f(x)-f(y)}{y-x}\frac{y}{f(y)} = -Df(y)\frac{y}{f(y)} \leq -Df(f(1/\beta))\frac{f(1/\beta)}{f^2(1/\beta)} < 1. \tag{10}$$

The last inequality follows from (7). Set

$$\mu = \max\Big\{\mu_1, -Df(f(1/\beta))\frac{f(1/\beta)}{f^2(1/\beta)}\Big\}, \tag{11}$$

then we have $\tau(x,y) < \mu$. □

Lemma 3.2. *Let γ and μ be as in the above Lemma. Fix $n \in \mathbb{Z}^+$, $\theta_0 \in \mathbb{S}^1$, $x_0, y_0 \in I$, and denote $(\theta_k, x_k) = F^k(\theta_0, x_0)$ and $(\theta_k, y_k) = F^k(\theta_0, y_0)$ for $k = 1, 2, \cdots, n-1$. Assume that $x_k, y_k \in (0, f(1/\beta)]$ for every $k \in \{0, 1, \cdots, n-1\}$. Then, $|x_n - y_n| \leq f(1/\beta)\mu^{m(n)}$, where $m(n)$ is the number of indices $k \in \{0, 1, \cdots, n-1\}$ such that $x_k, y_k \in [\gamma, f(1/\beta)]$.*

Proof. If $x_n = y_n$ then there is nothing to prove. Assume that $x_n \neq y_n$. Then also $x_k \neq y_k$ for $k = 0, 1, \ldots, n-1$. We have

$$\begin{aligned} \kappa(x_{k+1}, y_{k+1}) &= \frac{|x_{k+1} - y_{k+1}|}{\max\{x_{k+1}, y_{k+1}\}} = \frac{|f(x_k)\, g(\theta_k) - f(y_k)\, g(\theta_k)|}{\max\{f(x_k)\, g(\theta_k), f(y_k)\, g(\theta_k)\}} \\ &= \frac{|f(x_k) - f(y_k)|}{\max\{f(x_k), f(y_k)\}} = \kappa(f(x_k), f(y_k)). \end{aligned} \tag{12}$$

Therefore

$$\begin{aligned} |x_n - y_n| &\leq f\left(\frac{1}{\beta}\right) \kappa(x_n, y_n) = f\left(\frac{1}{\beta}\right) \kappa(x_0, y_0) \prod_{k=0}^{n-1} \frac{\kappa(x_{k+1}, y_{k+1})}{\kappa(x_k, y_k)} \\ &= f\left(\frac{1}{\beta}\right) \kappa(x_0, y_0) \prod_{k=0}^{n-1} \tau(x_k, y_k) \leq f\left(\frac{1}{\beta}\right) \prod_{k=0}^{n-1} \tau(x_k, y_k). \end{aligned} \tag{13}$$

Thus, by Lemma 3.1, we get $|x_n - y_n| \leq f\left(\frac{1}{\beta}\right) \mu^{m(n)}$. □

Lemma 3.3. *[12, Lemma 2]. Let $(X, \mathcal{F}, \mu)$ be a probability space, $T : X \to X$ a measurable transformation leaving the measure μ invariant, and $f : X \to \mathbb{R}$ a measurable function. If the function $f \circ T - f$ has a minorant $g \in \mathrm{L}^1_\mu$, then $f \circ T - f \in \mathrm{L}^1_\mu$ and*

$$\int (f \circ T - f) d\mu = 0.$$

Now we can prove the main result in this section.

Theorem 3.1. *When $2 < \alpha < 2e$, there exists a function $\zeta : \mathbb{S}^1 \to I$ such that*

(1) ζ is a measurable function and has an invariant graph;

(2) ζ is positive a.e.;

(3) ζ is discontinuous a.e.;

(4) the Lyapunov exponent in the x direction $\lambda_x(\zeta(\theta), \theta) < 0$ for a.e. $\theta \in \mathbb{S}^1$.

Proof. By Lemma 3.2, there exists a function $\zeta : \mathbb{S}^1 \to I$ which has an invariant graph. Taking a continuous function $\phi : \mathbb{S}^1 \to (0, f(1/\beta)]$, then $F^k(\phi)$ converges to ζ as $k \to \infty$. Therefore, ζ is a measurable function.

Since $f(0) = 0$, the set $\{\theta \in \mathbb{S}^1 : \zeta(\theta) = 0\}$ is invariant under rotation by ω. This implies that $\{\theta \in \mathbb{S}^1 : \zeta(\theta) > 0\}$ is also invariant under the same rotation. Moreover, $\lambda_x(0, \theta) > 0$ for a.e. $\theta \in \mathbb{S}^1$, $\theta \mapsto \theta + \omega$ preserves the Lebesgue measure on $\mathbb{S}^1$ and is ergodic, so $\{\theta \in \mathbb{S}^1 : \zeta(\theta) > 0\}$ has Lebesgue measure 1.

For every $\theta \in \mathbb{S}^1$ with $\zeta(\theta) > 0$, take a sequence $\{\theta_k\}$ such that $\zeta(\theta_k) = 0$ for all k and $\lim_{k\to\infty} \theta_k = \theta$, then $\lim_{k\to\infty} \zeta(\theta_k) = 0$. This implies that ζ is almost everywhere discontinuous. For example, we take $\omega = \frac{\sqrt{5}-1}{2}$, $\alpha = 2.2$ and $\beta = 2$, the attractor is everywhere discontinuous, as shown in Fig. 1.

By Birkhoff's ergodic theorem,

$$\lambda_x(\zeta(\theta), \theta) = \int_{\mathbb{S}^1} \log |Df(\zeta(\theta))| d\theta + \int_{\mathbb{S}^1} \log g(\theta) d\theta \tag{14}$$

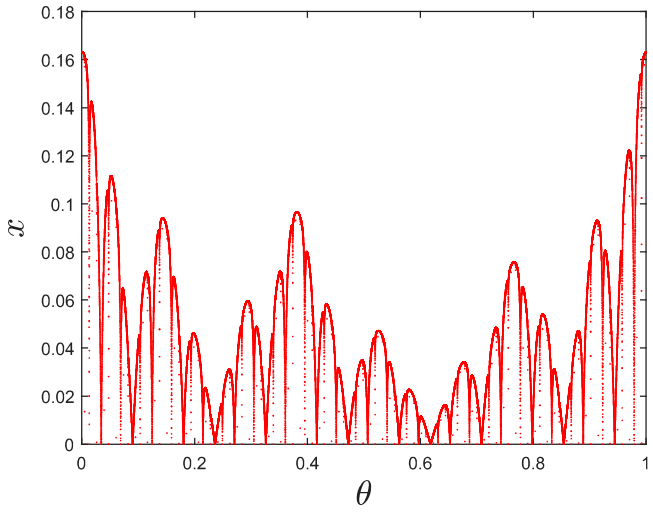

Figure 1: For $\alpha = 2.2$ and $\beta = 2$, the phase diagram in the plane (θ, x).

for a.e. $\theta \in \mathbb{S}^1$. Since $f(0) = 0$, $f(\zeta(\theta))g(\theta) = \zeta(\theta + \omega)$ and $Df(x) < \frac{f(x)}{x}$ for $0 < x \leq f(1/\beta)$,

$$|Df(\zeta(\theta))| < \frac{f(\zeta(\theta))}{\zeta(\theta)} = \frac{\zeta(\theta + \omega)}{\zeta(\theta)g(\theta)} \tag{15}$$

for a.e. $\theta \in \mathbb{S}^1$. Thus, $\log \frac{\zeta(\theta+\omega)}{\zeta(\theta)}$ has the integrable minorant $\log |Df(\zeta(\theta))| + \log g(\theta)$. Using Lemma 3.3, it follows that $\log \frac{\zeta(\theta+\omega)}{\zeta(\theta)}$ is integrable and $\int_{\mathbb{S}^1} \log \frac{\zeta(\theta+\omega)}{\zeta(\theta)} d\theta = 0$. Hence

$$\int_{\mathbb{S}^1} \log |Df(\zeta(\theta))| d\theta + \int_{\mathbb{S}^1} \log g(\theta) d\theta < \int_{\mathbb{S}^1} \log \frac{\zeta(\theta + \omega)}{\zeta(\theta)} d\theta = 0. \tag{16}$$

This proves $\lambda_x(\zeta(\theta), \theta) < 0$ for a.e. $\theta \in \mathbb{S}^1$. □

4. Numerical results

For $\omega = \frac{\sqrt{5}-1}{2}$, we will analyse the dynamical properties on the parameter set $\{(\alpha, \beta) | \alpha \in (1, 25], \beta \in [1, 5]\}$. Since the Lyapunov exponent in the x direction at $(0, \theta)$ is $\log \alpha - \log 2$, the attractive property of the x-axis is independent of the value β, see Fig. 2. For $\alpha \in (1, 2)$ (the white area), the attractors are quasiperiodic, the orbits shift irrationally on $\{(x, \theta) | x = 0, \theta \in [0, 1]\}$. The criterion is Lyapunov exponent $\lambda_x < 0$ in the x direction. For $\alpha \in [2, 16.5]$ (light grey area), the attractor is SNA. The criterion is Lyapunov exponent $\lambda_x < 0$, and that the phase sensitivity exponent does not tend to zero. For $\alpha \in [16.5, 19]$, the light grey and grey appear alternately, and the interval is the transition from SNA to chaotic attractor. For $\alpha \in [19, 25]$ (grey area), the attractor is a chaotic attractor, and the criterion is Lyapunov exponent $\lambda_x > 0$. For $\beta = 2$ and $\alpha \in [1, 25]$, the Lyapunov exponent λ_x in the x direction varies with the parameter α, as shown in Fig. 3. Its chaotic property corresponds to Fig. 2.

For $\beta = 2$, α is taken as the control parameter. The number of iterations is 50,000, discarding the first 20,000 iterations and then plotting the next 30,000 ones. For $1 <$

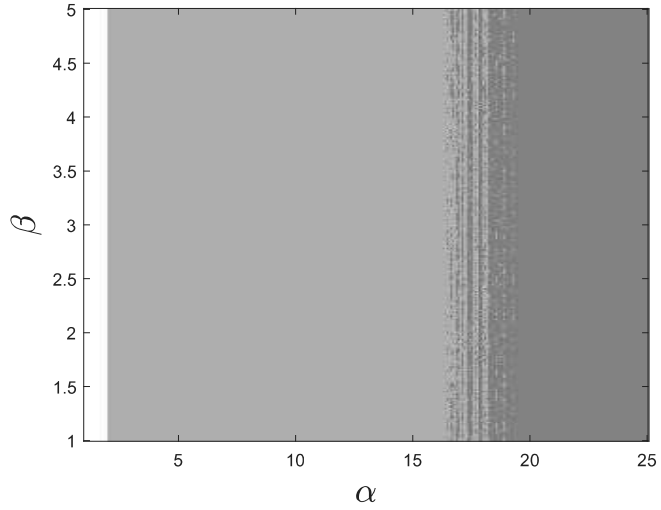

Figure 2: The phase diagram in the plane (α, β).

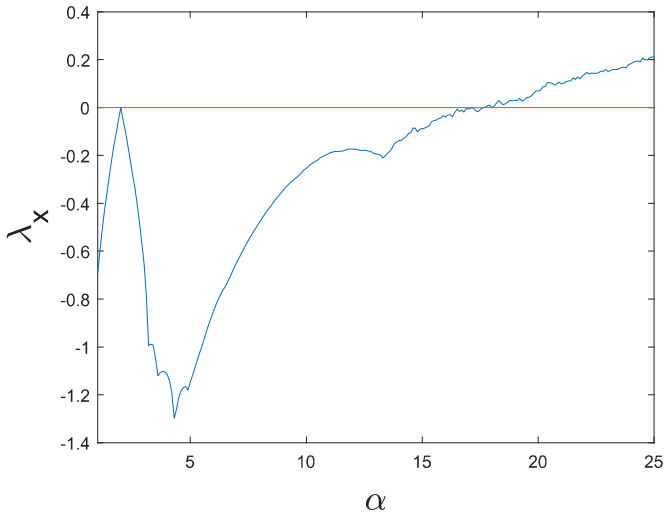

Figure 3: For $\beta = 2$ and $\alpha \in [1, 25]$, the Lyapunov exponent in the x direction.

$\alpha \leq 2$, the attractor is quasiperiodic, and the trajectory is attracted to the x-axis. For $2 < \alpha < 2e$, we proved that the attractor is SNA. When $2e \leq \alpha \leq 16.5$, SNAs still exist, see Fig. 2. Taking $\alpha = 15$ as an example, the attractor is nonsmooth and fractal, as shown in Fig. 4(a). The Lyapunov exponent in the x direction is $\lambda_x = -0.0935$, see Fig. 5(a), so the attractor is a SNA. When α is in the interval $[16.5, 19]$, SNAs alternate with chaotic attractors, there is a transition interval of parameter α in which SNAs are transformed into chaotic attractors. For $\alpha = 20$, the attractor becomes a chaotic attractor with Lyapunov exponent $\lambda_x = 0.0792$, as shown in Fig. 4(b) and Fig. 5(b).

4.1. Phase sensitivity property

The strange property can be effectively characterized by the phase sensitivity property [2].

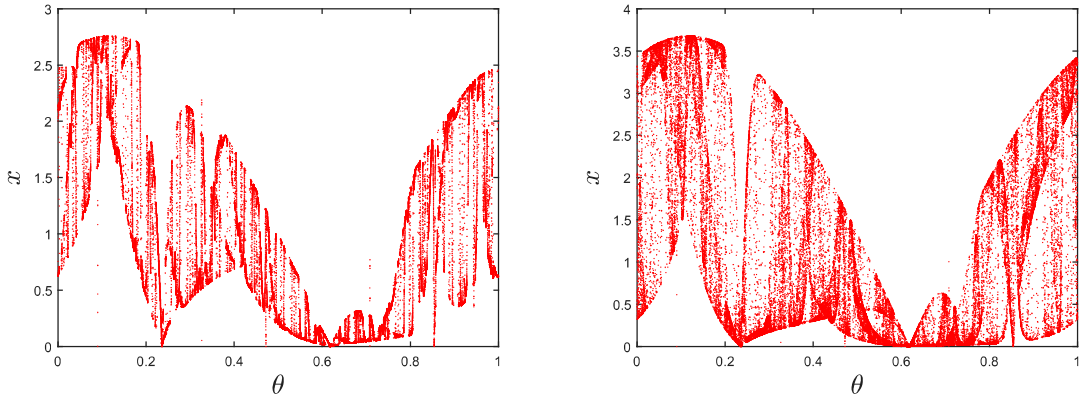

(a) $\alpha = 15$ (b) $\alpha = 20$

Figure 4: For $\beta = 2$, the phase diagram in the plane (θ_n, x_n). (a) SNA, (b) chaotic attractor.

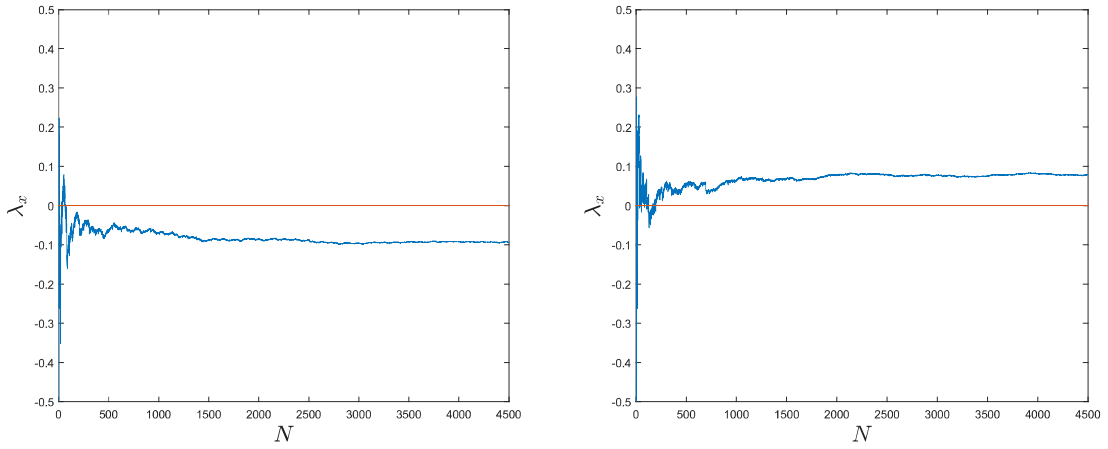

(a) (b)

Figure 5: The Lyapunov exponent in the x direction. (a) $\alpha = 15, \beta = 2$, (b) $\alpha = 20, \beta = 2$.

From the map F we get the recurrence relation

$$\begin{aligned} \frac{\partial x_{n+1}}{\partial \theta} &= F_\theta\left(x_n, \theta_n\right) + F_x\left(x_n, \theta_n\right) \frac{\partial x_n}{\partial \theta} \\ &= \pi\alpha x_n e^{-\beta x_n} \cos(\pi\theta_n) + \alpha(1 - \beta x_n) e^{-\beta x_n} \sin(\pi\theta_n) \frac{\partial x_n}{\partial \theta_n}. \end{aligned} \tag{17}$$

Thus, starting from the initial derivative $\frac{\partial x_n}{\partial \theta}$, we get derivatives at all points of the trajectory:

$$\begin{aligned} \frac{\partial x_N}{\partial \theta} &= \sum_{k=1}^{N} F_\theta\left(x_{k-1}, \theta_{k-1}\right) R_{N-k}\left(x_k, \theta_k\right) + R_N\left(x_0, \theta_0\right) \frac{\partial x_n}{\partial \theta} \\ &= \sum_{k=1}^{N} \pi\alpha x_{k-1} e^{-\beta x_{k-1}} \cos\left(\pi\theta_{k-1}\right) R_{N-k}\left(x_k, \theta_k\right) + R_N\left(x_0, \theta_0\right) \frac{\partial x_n}{\partial \theta}, \end{aligned} \tag{18}$$

where

$$R_M\left(x_m,\theta_m\right)=\prod_{i=0}^{M-1}F_x\left(x_{m+i},\theta_{m+i}\right)=\prod_{i=0}^{M-1}\alpha\left(1-\beta x_{m+i}\right)e^{-\beta x_{m-i}}\sin\left(\pi\theta_{m+i}\right), \tag{19}$$

$R_0=1$ and N is the number of iterations. According to Ref. [2], $R_N\approx\pm\exp\left(\lambda_x N\right)$. If the attractor is not chaotic as $N\to+\infty$ then $\lambda_x<0$, and $R_N(x_0,\theta_0)\frac{\partial x_0}{\partial\theta}$ is a small quantity. Then the equation (4) can be expressed as

$$\frac{\partial x_N}{\partial\theta}\approx S^N=\sum_{k=1}^{N}F_\theta(x_{k-1},\theta_{k-1})R_{N-k}(x_k,\theta_k). \tag{20}$$

If S^N tends to infinite as $N\to+\infty$ then the attractor is nonsmooth, which characterizes the attractor to be strange.

The maximum value of S^N after N iterations is denoted by

$$\tau^N=\max_{1\le i\le N}\{S^i\}. \tag{21}$$

According to Ref. [2], we know $\gamma_N=\min_{x,\theta}\tau_N(x,\theta)$ and $\gamma_N\approx N^\mu$, where μ is called the phase sensitivity exponent. If the number of iterations increases, the value of τ^N increases accordingly. If S^N tends to infinite with $N\to+\infty$ then the attractor has infinite derivative with respect to the phase θ. In such a case, the attractor is strange.

Taking SNA ($\beta=2$ and $\alpha=15$) in Fig. 4(a) as an example. According to Eqs. (20) and (21), τ^N is the maximum derivative of x with respect to the phase θ, and μ is the phase sensitivity exponent. For $\alpha=15$, the attractor is a SNA. If the attractor is smooth, τ^N is bounded and the phase sensitivity exponent μ tends to zero. If the attractor is nonsmooth, τ^N tends to infinite and the phase sensitivity exponent μ is not equal to zero. We choose the parameter $\beta=2$, and $\alpha=1.5$ (quasiperiodic attractor) and $\alpha=15$ (SNA, as shown in Fig. 4(a)). In the numerical calculation, 10,000 iterations and 100,000 iterations are selected to obtain the change image of τ^N with the number of iterations, see Figs. 6(a) and 6(b). In Figs. 6 ($\alpha=1.5$), it is shown that when the attractor is quasiperiodic, the value of τ^N approximates a horizontal line and tends to a bounded value, and the phase sensitivity exponent μ tends to zero. When the attractor is a SNA ($\alpha=15$), as the number of iterations increases, the value of τ^N increases continuously. For $10,000$ iterations and $100,000$ iterations, the phase sensitivity exponent is $\mu=1.3319$ and $\mu=1.4132$, respectively. When N tends to infinite, τ^N also tends to infinite, which means that the attractor is everywhere nonsmooth (i.e. strange).

4.2. Rational approximations

Rational approximations is also an effective method to characterize the strange properties of SNAs [2]. When ω is equal to the golden mean value, the ratios of Fibonacci numbers ($\omega_k=F_{k+1}/F_k, F_{k+1}=F_k+F_{k-1}, F_1=1, F_2=1$) are approximations. We also take the SNA in Fig. 4(a) ($\beta=2$ and $\alpha=15$) as an example, and choose the approximations $\omega_{10}=34/55, \omega_{16}=610/987, \omega_{19}=4181/6765$ and $\omega_{21}=10946/17711$. For $k=10$ or 16, the approximation order is low, and there are only some periodic points in the phase diagram of the plane (θ_n, x_n). The fractal structure of SNA can not be observed, see Figs. 7. When the approximation order is high ($k=19$ or 21), the phase diagram in the plane

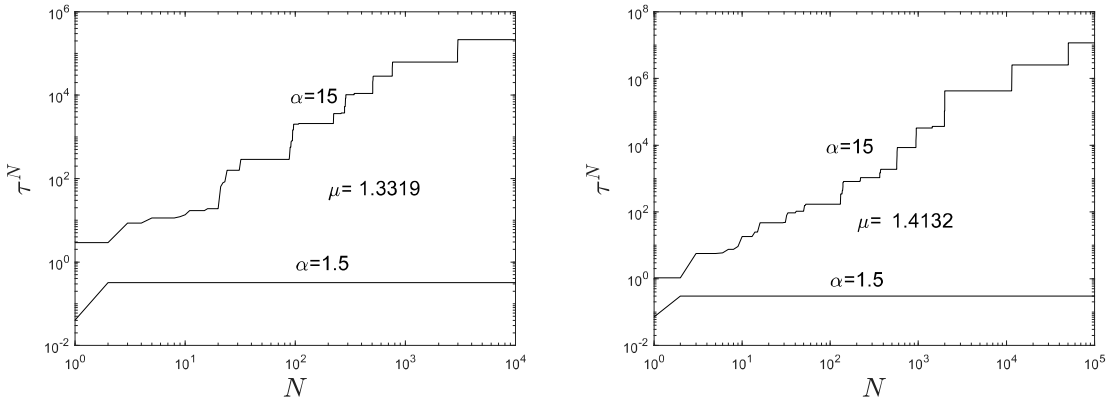

Figure 6: Phase sensitivity functions: (a) 10,000 iterations, (b)100,000 iterations.

(θ_n, x_n) approximates the geometric fractal structure of Fig. 4(a), as shown in Figs. 7(c) and 7(d). In Figs. 7, it is shown that as the order of approximation increases, the number of periodic points also increases. For $k \to +\infty$, the number of periodic points in the phase diagram tends to be infinite and the structure of the attractor is nonsmooth, which can approximate the strange nonchaotic property of the original quasiperiodic system.

5. Conclusion

In this paper, we investigate SNAs in the Ricker family with quasiperiodic excitation, and determine the parameter region in which SNAs exist by combining mathematical proofs with numerical calculations. Our discussions are divided into two parts. First, we use theoretic methods to prove the existence of SNAs in some parameter region. Our results show that the SNAs are discontinuous almost everywhere in such parameter region. Besides, we also use precise numerical methods to explain the existence of SNAs in a larger parameter region. We also find that there is a transition region in which SNAs alternate with chaotic attractors. The main numerical methods include the evaluation of Lyapunov exponents, phase sensitivity and rational approximations.

Acknowledgments

This work is supported by the National Natural Science Foundation of China (11672249, 11732014 and 11572263).

References

[1] Grebogi, C., Ott, E., Pelikan, S., Yorke, J.A.: Strange attractors that are not chaotic. Physica D, 1984, 13: 261-268.

[2] Pikovsky, A.S., Feudel, U.: Characterizing strange nonchaotic attractors. Chaos, 1995, 5(1): 253-260.

[3] Jalnine, A.Y., Kuznetsov, S.P.: Autonomous strange nonchaotic oscillations in a system of mechanical rotators. Regular and Chaotic Dynamics, 2017, 22(3): 210-225.

[4] Zhang, Y.: Wada basins of strange nonchaotic attractors in a quasiperiodically forced system. Physics Letters A, 2013, 377(18): 1269-1273.

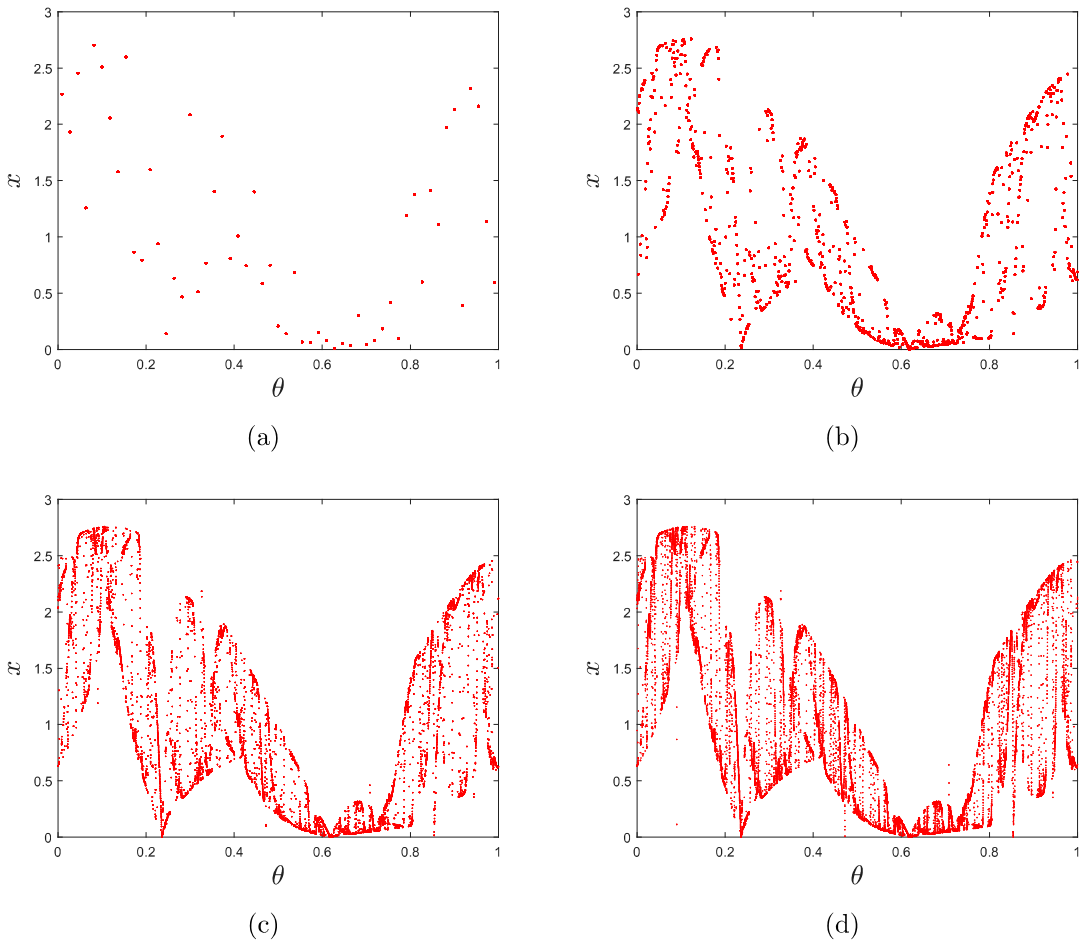

Figure 7: Rational approximations, where $\beta = 2$, $\alpha = 15$. (a) $\omega_{10} = 34/55$, (b) $\omega_{16} = 610/987$, (c) $\omega_{19} = 4181/6765$, (d) $\omega_{21} = 10946/17711$.

[5] Jorba, A., Munoz-Almaraz, F.J., Tatjer, J.C.: On non-smooth pitchfork bifurcations in invertible quasi-periodically forced 1-D maps. Journal of Difference Equations and Applications, 2017:1-21.

[6] Zhou, T., Moss, F., Bulsara, A.: Observation of a strange nonchaotic attractor in a multistable potential. Physical Review A 45, 5394C5400 (1992)

[7] Sivaganesh, G., Sweetlin, M.D., Arulgnanam, A.: Synchronization of strange non-chaotic attractors via unidirectional coupling of quasiperiodically-forced systems. Journal of the Korean Physical Society, 2016, 69(2): 124-130.

[8] Ding, M., Grebogi, C., Ott, E.: Dimensions of strange nonchaotic attractors. Physics Letters A, 1989, 137(4): 167-172.

[9] Ding, M., Grebogi, C., Ott, E.: Evolution of attractors in quasiperiodically forced systems: From quasiperiodic to strange nonchaotic to chaotic. Physical Review A, 1989, 39(5): 2593-2598.

[10] Ditto, W.L., Spano, M.L., Savage, H.T., Rauseo, S.N., Heagy J.F Ott E.: Experimental observation of a strange nonchaotic attractor. Physical Review Letters. 65, 533C536 (1990).

[11] Aravindh, M.S., Venkatesan, A., Lakshmanan, M.: Strange nonchaotic attractors for computation. Physical Review E, 2018, 97(5): 052212.

[12] Keller, G.: A note on strange nonchaotic attractors. Fundamenta Mathematicae. 1996, 151: 139-148.

[13] Alsedà, L., Misiurewicz, M.: Attractors for unimodal quasiperiodically forced maps. Journal of Difference Equations and Applications, 2008, 14(10-11): 1175-1196.

[14] Glendinning, P., Jäeger, T., Keller, G.: How chaotic are strange nonchaotic attractors. Nonlinearity, 2006, 19(9): 2005-2022.

[15] Jäeger, T.H.: On the structure of strange non-chaotic attractors in pinched skew products. Ergodic Theory and Dynamical Systems, 2013, 27(2): 493-510.

[16] Premraj, D., Suresh, K., Palanivel, J., et al.: Dynamic bifurcation and strange nonchaos in a two frequency parametrically driven nonlinear oscillator. Communications in Nonlinear Science and Numerical Simulation, 2017, 50: 103-114.

[17] Thamilmaran, K., Senthilkumar, D.V., Venkatesan, A., Lakshmanan, M.: Experimental realization of strange nonchaotic attractors in a quasiperiodically forced electronic circuit. Physical Review E. 2006, 74: 036205.

[18] Heagy, J., Ditto, W.L.: Dynamics of a two-frequency parametrically driven duffing oscillator. Journal of Nonlinear Science, 1991, 1(4): 423-455.

[19] Nishikawa, T., Kaneko, K.: Fractalization of torus revisited as a strange nonchaotic attractor, Phys. Physical Review E Statistical Physics Plasmas Fluids and Related Interdisciplinary Topics, 1996, 39(54): 6114-6124.

[20] Kim, J.W., Kim, S.Y., Hunt, B., et al.: Fractal properties of robust strange nonchaotic attractors in maps of two or more dimensions. Physical Review E, 2003, 67(3): 036211.

[21] Hunt, B.R., Ott, E.: Fractal Properties of Robust Strange Nonchaotic Attractors. Physical Review Letters, 2001, 87(25): 254101.

[22] Shen, Y., Zhang, Y.: Strange nonchaotic attractors in a quasiperiodically forced piecewise smooth system with Farey tree. Fractals, 2019, 27: 1950118.

[23] Heagy, J.F., Hammel, S.M.: The birth of strange nonchaotic attractors. Physica D, 1994, 70(1-2): 140-153.

[24] Prasad, A., Mehra, V., Ramaswamy, R.: Intermittency Route to Strange Nonchaotic Attractors. Physical Review Letters, 1997, 79(21): 4127-4130.

[25] Venkatesan, A., Murali, K., Lakshmanan, M.: Birth of strange nonchaotic attractors through type III intermittency. Physics Letters A, 1999, 259(3-4): 246-253.

[26] Kim, S. Y., Lim, W., Ott, E.: Mechanism for the Intermittent Route to Strange Nonchaotic Attractors. Physical Review E, 2003, 67(5): 056203.

[27] Shen, Y., Zhang, Y.: Mechanisms of strange nonchaotic attractors in a nonsmooth system with border-collision bifurcations. Nonlinear Dynamics, 2019, 96: 1405-1428.

[28] Li, G., Yue, Y., Xie, J., Grebogi, C.: Strange nonchaotic attractors in nonsmooth dynamical system. Communications in Nonlinear Science and Numerical Simulation, 2019, 78: 104858.

[29] Arulgnanam, A., Prasad, A., Thamilmaran, K., Daniel, M.: Multilayered bubbling route to SNA in a quasiperiodically forced electronic circuit with experimental and analytical confirmation. Chaos Soliton Fractals, 2015, 75: 96C110.

[30] Suresh, K., Prasad, A., Thamilmaran, K.: Birth of strange nonchaotic attractors through formation and merging of bubbles in a quasiperiodically forced Chuas oscillator. Physics Letters A. 2013, 377: 612C621.

[31] Lindner, J.F., Kohar, V., Kia, B., Hippke, M., Learned, J.G., Ditto, W.L.: Strange Nonchaotic Stars. Physical Review Letters, 2015, 114(5): 054-101.

[32] Zelinka, I., Kojecky, L., Senkerik, R.: Strange Nonchaotic Attractors in Evolutionary Processing of Astroinformatic Big Data. 2016 Fifteenth Mexican International Conference on Artificial Intelligence (MICAI). IEEE Computer Society, 2016.

[33] Yue, Y., Miao, P., Xie, J.: Coexistence of strange nonchaotic attractors and a special mixed attractor caused by a new intermittency in a periodically driven vibro-impact system. Nonlinear Dynamics, 2017, 87(2): 1-21.

[34] Zhang, Y., Luo, G.: Torus-doubling bifurcations and strange nonchaotic attractors in a vibro-impact system. Journal of Sound and Vibration, 2013, 332(21): 5462-5475.

[35] Wang, X., Zhan, M., Lai, C.H., et al.: Strange nonchaotic attractors in random dynamical systems. Physical Review Letters, 2004, 92(7): 074-102.

[36] Wang, X., Lai, Y.C., Lai, C.H.: Characterization of noise-induced strange nonchaotic attractors. Physical Review E, 2006, 74(1): 016203.